

# Structure of A=138 isobars above the $^{132}\text{Sn}$ core and the N-N interaction in the neutron-rich environment

S. Sarkar

*Department of Physics, Bengal Engineering and Science University,  
Shibpur, Howrah - 711103, INDIA.*

M. Saha Sarkar

*Nuclear and Atomic Physics Division,  
Saha Institute of Nuclear Physics, Kolkata 700064, INDIA*

(Dated: November 11, 2018)

## Abstract

Large basis untruncated shell model calculations have been done for the A=138 neutron -rich nuclei in the  $\pi(gdsh) \oplus \nu(hfpi)$  valence space above the  $^{132}\text{Sn}$  core. Two (1+2) -body nuclear Hamiltonians, viz., realistic CWG and empirical SMPN in this model space have been used. Calculated ground state binding energies, level spectra and other spectroscopic properties have been compared with the available experimental data. Importance of untruncated shell model calculations in this model space has been pointed out. Shell model results for the very neutron rich Sn isotope ( $^{138}\text{Sn}$ , N/Z=1.76) of astrophysical interest for which no spectroscopic information except  $\beta$  -decay half life is available, have been presented. Shell structure and evolution of collectivity in the even-even A=138 isobars have been studied as a function of valence neutron and /or proton numbers. Calculations done for the first time, reproduce remarkably well the collective vibrational states in  $^{138}\text{Te}$  and  $^{138}\text{Xe}$ . Comparison of some of the important two-body matrix elements of the empirical SMPN, CW5082 and the realistic CWG interactions has been done. These matrix elements are important for ground state binding energies and low-lying spectra of nuclei in this region. Consideration of the predictability of the two interactions seems to suggest that, in order to incorporate the special features of the N-N interaction in such exotic n-rich environment above the  $^{132}\text{Sn}$  core, the use of local spectroscopic information from the region might be essential.

PACS numbers: 21.60.Cs,21.30.Fe,21.10.Dr,23.20.Lv,23.20.Js,27.60.+j,

## I. INTRODUCTION

Recent experimental and theoretical investigations in the close-to-neutron-drip line region above the doubly magic  $^{132}\text{Sn}$  nucleus have revealed many intriguing issues concerning some newer aspects of nuclear structure and empirical / realistic N-N interaction in such exotic environments. Decrease in the spin-orbit interaction at N-Z=32 above the Z=50, N=82 double shell closure [1], anomalously low excitation energy (282 keV) of the first  $5/2^+$  state in the  $^{135}\text{Sb}$  compared to its position in  $^{133}\text{Sb}$  (962 keV) [2], anomalously low  $B(E2, 0_{gs}^+ \rightarrow 2_1^+)$  value in  $^{136}\text{Te}$  [3], the question of appearance of deformation and the locus of transition from single particle to collective behaviour, as well as the evolution of collectivity in these neutron-rich nuclei above  $^{132}\text{Sn}$  core and the role therein of the number of valence neutrons and protons, are some of the structure issues being studied recently. The question of reduced neutron-neutron pairing in the exotic n-rich environment [4] above N=82 [5], and modification of the empirical / effective two-body matrix elements (tbmes) in the valence space ( $\pi g d s h, \nu h f p i$ ) above the  $^{132}\text{Sn}$  core for shell model applications, are also of current interest. Moreover nuclei with  $50 \leq Z \leq 56$  and  $82 \leq N \leq 88$  lie on or close to the path of the astrophysical r-process flow. Thus the knowledge of the structure, particularly the binding energies, low - lying excited states and  $\beta$ -decay rates of these nuclei at finite temperatures, are important ingredients for investigation in the nucleosynthesis scenario. However, many of these important nuclei are yet to be studied experimentally. For example, the even-N neutron-rich Sn isotopes are the classical "waiting point" nuclei in the A=130 solar system abundance peak under typical r-process conditions. With respect to the r-process,  $^{136}\text{Sn}$  is an important waiting -point nucleus for moderate neutron densities to drive the r-process flow beyond A $\simeq$ 130 peak [6]. Some spectroscopic information, such as binding energy and low -lying spectrum exist only for the  $^{134}\text{Sn}$ . Recently, the  $\beta$ -decay half lives via delayed neutron emission have been measured for  $^{135}\text{Sn}$  to  $^{138}\text{Sn}$  nuclei [6]. Their production rates and lifetimes are small. This provides severe limitations in acquiring spectroscopic information on them. Therefore, reliable theoretical calculations and their comparisons with the hitherto available experimental data on the binding energies, level spectra, electromagnetic properties and  $\beta$  -decay rates are not only important for extending our knowledge of N-N interaction and nuclear structure in the exotic n-rich environment, but they also provide very useful ingredients for reviewing the problems related to the nuclear astrophysics in

general.

Theoretical studies in the framework of nuclear shell model (SM) have been done [7, 8, 9, 10, 11, 12, 13, 14, 15, 16, 17, 18] recently for these nuclei above the  $^{132}\text{Sn}$  core in the valence space consisting of  $\pi(1g_{7/2}, 2d_{5/2}, 2d_{3/2}, 3s_{1/2}, 1h_{11/2})$  and  $\nu(1h_{9/2}, 2f_{7/2}, 2f_{5/2}, 3p_{3/2}, 3p_{1/2}, 1i_{13/2})$  orbitals. These SM calculations using realistic [9, 13, 14, 18] and empirical [7, 8, 10, 11, 12, 15, 16, 17] interactions in this valence space yield remarkably good results for some of the isotopes of Sn, Sb, Te, I, Xe, Cs. The empirical SMPN [8, 10] interaction, applied for all the nuclei in the range  $134 \leq A \leq 138$  and  $50 \leq Z \leq 56$  are found to be highly successful [10] in predicting particularly the ground state spin-parities, binding energies, level spectra and electromagnetic transition probabilities. In a recent work [10] we have identified that a mild collectivity appears in the  $^{137}\text{I}, \text{Te}$  [19, 20] nuclei with  $N = 84$  and  $85$ , respectively. The spectra of  $^{138}\text{Te}$  [21],  $^{138}\text{Xe}$  [22] and  $^{139}\text{I}$  [23, 24] also showed good vibrational characteristics. Because of the computational limitations we then studied the evolution of collectivity in the odd- $A$  nuclei for  $N=84-87$  with Particle-Rotor Model [25] and indicated the role played by the valence protons and neutrons in them. The role of the valence protons and neutrons have been also studied in the context of the structure of  $^{138}\text{I}$  and  $^{138}\text{Cs}$  [16, 17]. It has been found that the single particle behaviour persists for nuclei with neutrons only in the valence space up to at least  $N=87$ . The calculated results for the spectroscopic information on  $^{136,137}\text{Sn}, \text{Sb}$  isotopes have been reported already in Ref.[10, 12]. The present work is motivated to discuss the results of untruncated shell model calculations over the  $\pi(gdsh) \oplus \nu(hfpi)$  valence space on the spectroscopic properties of the  $A=138$  even-even isobars and to study the evolution of collectivity in these nuclei using the code OXBASH [26]. It is expected to reveal the role of valence nucleon species on the evolution of collectivity. The other motivation is to compare the results of SM calculations with SMPN interaction [10] with those with the CD-Bonn potential based realistic CWG [14] interaction used in this region. The theoretical results have also been compared with the experimental data, wherever available. We have then compared the two sets of two-body interaction matrix elements to gain insight in to the N-N interaction for this n-rich environment.

## II. SHELL MODEL RESULTS AND DISCUSSIONS

The calculations were carried out in the z50n82 model space with the SMPN [10] and CWG Hamiltonians [14] using the code OXBASH [26].

We started [27] our shell model calculations for the  $^{138}\text{Sn}$  nucleus in a slightly truncated space excluding the intruder  $1i_{13/2}$  neutron orbital. This was done on the observation of very small (2-5%) contributions of particle-partitions involving this orbital in the  $^{136-137}\text{Sn}$  wavefunctions. No signature of any collective feature of the states was found with the increasing neutron number in the N=84-88 isotopes of Sn. Shell model results with the SMPN (1+2) body Hamiltonian were encouraging for these n-rich Sn isotopes. It was noted that an estimate [23] of the energy of the first  $2^+$  excited state in  $^{136}\text{Sn}$  was at 600 keV. The calculated result for this was at 578 keV. Similarly, the systematically estimated [23] energy value of the  $11/2^+$  level in  $^{137}\text{Sn}$  was  $\approx 600$  keV and the calculated value was 550 keV. The estimated [23] energy of the second  $5/2^+$  level in  $^{137}\text{Sb}$  was also closer to the calculated result at 773 keV.

With the availability of the window version of the OXBASH [26] and Nushell@MSU [28] codes, it became possible for us to perform untruncated shell model calculations including the  $\nu 1i_{13/2}$  orbital, for all the A=138 isobars with six valence particles in the large basis space of 76 single particle states mentioned above. The effect of the inclusion of this intruder orbital in the model space has been presented in Table I. It shows the importance of the full basis calculation. Substantial changes in the ground state binding energy and excitation energies of the yrast levels in the spectrum of  $^{138}\text{Sn}$  can be noted. Although the average percentage changes in the absolute binding energies of the states are  $\simeq 2\%$ , the resultant effect on the excitation energy spectrum is dramatic. Wave function compositions of the states for both the calculations are also given in the Table. Comparison of the wave functions of the same state of the two calculations shows that they do not differ much. This is reflected in the  $B(E2, 0_{gs}^+ \rightarrow 2_1^+)$  values of the two calculations, they differ, but not drastically. The results in Table I are from the SM calculations with the SMPN interaction.

### A. Comparison with systematics

In Figs. 1-4 experimental energy values of different states (yrast  $2^+$ ,  $4^+$ ,  $6^+$ ) for the even-even isotonic series of  $N=70-80$ ,  $84-88$  and isotopic series of  $Z=50-60$  are plotted. As for  $^{136}\text{Sn}$  and  $^{138}\text{Sn}$ , experimental level energy values are not available, we have plotted the predicted values from our calculations using SMPN (Fig.1) and CWG (Fig.2). Calculated energies for the first  $2^+$  levels ( $E(2_1^+)$ ) in  $^{136,138}\text{Sn}$ , using SMPN fit nicely in the systematics for  $N>82$  (Fig.1). The  $E(2_1^+)$  values calculated for Sn isotopes above  $N=82$  decreases with increasing neutron number. But the predicted  $E(2_1^+)$  values from the calculations using the CWG Hamiltonian, deviate sharply from the systematics for  $N>82$  (Fig.2). However these values agree with the feature observed for even - even (e-e) Sn isotopes below the  $^{132}\text{Sn}$  core. For CWG, the  $E(2_1^+)$  excitation energies for all the even-even Sn isotopes with  $N\geq 84$  are almost constant similar to those below  $N=82$ . Only difference is that the bunching of  $E(2_1^+)$  values now occur at around 750 keV for  $N\geq 84$  instead of 1200 keV for  $N\leq 82$ .

It thus seems that the CWG tbmes still carry the characteristic features of the not-so-neutron-rich domain below  $N=82$ . But the SMPN incorporates features of the exotic n-rich domain above the  $^{132}\text{Sn}$  core in some of its important tbmes appropriate for describing low-lying states for nuclei in this region, and its prediction for low energy eigenvalues seems to be more reliable, as is evidenced by the trend in the systematics. Similar observation is made from the Figs. 3a,b showing the variation of the ( $E(2_1^+)$  and  $E(4_1^+)$ ) of the isotopic series of  $Z=50$  to  $60$  with neutron numbers ranging from  $70$  to  $88$ . The Figs. 3a,3b show the results for Sn with  $N=86$  and  $88$  from SMPN and CWG calculations, respectively. The experimental energies of Sn isotopes stand out from the rest of the nuclei for  $N<82$  with nearly constant values of  $E(2_1^+)$  and  $E(4_1^+)$  from  $N=70$  to  $80$  with a very slow increasing trend with decreasing neutron number. In contrast, for other isotopic series  $E(2_1^+)$  and  $E(4_1^+)$  energies increase slowly with increasing neutron number and become largest at  $N=82$  and then decrease again for  $N>82$ . But for  $N>82$ , the variation as predicted with both SMPN and CWG changes dramatically. The SMPN results totally match with the local systematics. The CWG still retains the near constancy but with much reduced values, with a slight increasing trend with increasing neutron number. It seems that for  $N<82$ , the Sn isotopes were different from the rest due to their strong  $Z=50$  proton shell closed structure. But above  $N=82$ , the  $Z=50$  closure becomes weak and the special feature disappears. This

feature is corroborated by both theoretical results. However CWG results for Sn show that the variations of experimental  $E(2_1^+)$  and  $E(4_1^+)$  with neutron number have opposite slopes for  $N > 82$  compared to SMPN behaviour. Fig 4 shows the variation of  $E(2_1^+)$ ,  $E(4_1^+)$  and  $E(6_1^+)$  for  $N=84, 86$  and  $88$  for  $Z=50-60$ . The results from SMPN and CWG (for  $N=86,88$ ) are shown in the Figure. How the results match with the systematics of the isotones and also with the trend of  $N=84$  are evident. The SMPN results fit smoothly in the trend and also follow more closely the trend set by  $^{134}\text{Sn}$ . For the CWG results,  $Z=50$  proton shell closure seems to prevail in a comparatively stronger way.

## B. Sn isotopes

We now address the issue of the evolution of collectivity in the even-even  $^{134-138}\text{Sn}$  isotopes using SMPN [10] and CWG interactions from B.A. Brown *et al.*[14]. In Table II, energies, wavefunctions and  $B(E2, 0_{gs}^+ \rightarrow 2_1^+)$  have been compared for the yrast  $0^+$  and  $2^+$  states of the three Sn isotopes. As pointed out, the  $E(2_1^+)$  value decreases with increasing neutron number for SMPN, but remains almost constant for the CWG Hamiltonian. Structure of these states including the  $B(E2, 0_{gs}^+ \rightarrow 2_1^+)$  values, as shown in Table II, as well as the  $R_4 (= E_{4_1^+}/E_{2_1^+})$  values suggest that in the calculations using CWG, the  $^{136,138}\text{Sn}$  isotopes show a trend of gradual onset of collectivity. This is demonstrated by the mild increase in configuration mixing in the wavefunctions compared to the SMPN case and an increasing trend in the  $B(E2, 0_{gs}^+ \rightarrow 2_1^+)$  values. The  $R_4$  value is also close to 2 ( $R_4=1.78$ ) for  $^{138}\text{Sn}$  with CWG. But with SMPN, results are different,  $(\nu 2f_{7/2}^n)^{n=2,4,6}$  multiplet configuration is dominant for the two states in all these isotopes. The value of  $R_4$  is 1.70 for  $^{138}\text{Sn}$  with SMPN. Although the  $E(2_1^+)$  values are relatively smaller than those predicted by CWG, the structure of the wavefunctions and the  $B(E2, 0_{gs}^+ \rightarrow 2_1^+)$  values show the characteristics of single particle behaviour. This is a feature already observed experimentally in the n-rich  $^{136}\text{Te}$  isotope [3]. The anomalously low  $B(E2, 0_{gs}^+ \rightarrow 2_1^+)$  value found in this nucleus compared to that expected from the phenomenological modified Grodzin formula ( $B(E2, 0_{gs}^+ \rightarrow 2_1^+) \propto E_{2_1^+}^{-1}$ ) has drawn the attention of the community [5, 8, 10, 29]. Terasaki *et al.* [5] have traced this anomalous behaviour in the Te isotopes to a reduced neutron pairing above the  $N=82$  shell gap. This is consistent with the reduced diagonal n-n tbnms of the SMPN interaction [8, 10] discussed in Section III of this paper. It seems to be a unique

feature observed in neutron-rich nuclei. In this domain comparatively lower value of  $E(2_1^+)$  does not necessarily lead to a larger  $B(E2)$  value indicating collectivity.  $^{136}\text{Te}$  probably was the first nucleus for which this feature was identified [3]. Interestingly, similar behaviour is also seen near the  $N=20$  shell closure for neutron-rich  $\text{Mg}$  and  $\text{Ne}$  isotopes and also in the odd- $A$   $^{69-71}\text{Cu}$  isotopes [31].

Despite being a singly closed shell nucleus, in  $^{32}_{12}\text{Mg}_{g20}$ , the  $E(2_1^+)$  is 885 keV, much lower than that in the well deformed  $^{24}\text{Mg}$  ( $E(2_1^+)=1369$  keV). But the  $B(E2, 0_{gs}^+ \rightarrow 2_1^+)$  in  $^{32}\text{Mg}$  is only  $\simeq 13$  W.u compared to  $\simeq 21$  W.u. for  $^{24}\text{Mg}$  [30].

It has been pointed out in one of the recent work [25] that there are indications that the appearance of collectivity in the yrast levels occurs for nuclei with more than one neutron and proton in the valence space above the  $^{132}\text{Sn}$  core. But it is still not very clear how the onset and evolution of collectivity in these n-rich nuclei exactly depend on the number of valence neutrons and protons. So a microscopic investigation using shell model is indeed necessary and useful.

### C. Even-even $A=138$ isobars

We have studied the locus of evolution [21] of collectivity as a function of neutron and proton numbers. Our observation regarding this issue of evolution of collectivity in the low-lying yrast states in all the nuclei in range ( $Z=50-56$ ,  $N=82-88$ ) above the  $^{132}\text{Sn}$  core has been reported in ref. [32]. It is found that for nuclei with more than one neutron and one proton in the valence space, mild deformation appears at  $N=84, 85$ , i.e. even before  $N=87$ , and deformation / collectivity grows with increasing  $N$  and  $Z$ .

Shell model results for the  $^{138}\text{I}$ ,  $\text{Cs}$  nuclei have already been discussed elsewhere [16, 17]. These odd-odd isobars have excitation spectra, which are characteristic of spherical nuclei.

Here the results for only the even-even  $A=138$  isobaric series above the  $^{132}\text{Sn}$  core have been presented. The nuclei considered are  $^{138}\text{Sn}$  ( $T_z=+3.0$ ) with 6 neutrons,  $^{138}\text{Te}$  ( $T_z=+1.0$ ) with 4 neutrons and 2 protons,  $^{138}\text{Xe}$  ( $T_z=-1.0$ ) with 2 neutrons and 4 protons and finally,  $^{138}\text{Ba}$  ( $T_z=-3.0$ ) with 6 valence protons. Untruncated shell model calculations for 6 valence nucleons in this large basis space usually involve matrices of large dimensions, especially for nuclei having both neutrons and protons with comparable numbers or for those having relatively more neutrons (because of the  $\nu 1i_{13/2}$  orbital). The dimensions of the ma-

trices involved for different yrast ( $J^\pi, T$ ) - states of a particular  $A=138$  isobar are shown in Table III. Calculations for  $^{138}\text{Te}$  with 2 protons and 4 neutrons involve matrices of largest dimensions for a particular spin state.

### 1. Excitation spectra

For all these  $A=138$  nuclei, except  $^{138}\text{Sn}$ , excitation spectra are known. Calculated energy eigenvalues of the level spectra using both SMPN and CWG Hamiltonians are compared with the experimental data in Figs.(5-8). Calculated energy values of the levels with the SMPN Hamiltonian are in excellent agreement with experimental ones up to the highest observed level in  $^{138}\text{Te}$  (Fig.6) and  $^{138}\text{Xe}$  (Fig.7) (including the non-yrast levels in  $^{138}\text{Xe}$ , not shown in the figure). The agreement for CWG results is also very good in both the cases but all the energy eigenvalues of the excited states are systematically underpredicted by about 100-150 keV. The calculations remove the ambiguity of the spin-parity assignment of the second  $8^+$  state in  $^{138}\text{Te}$ . From the observed as well as the calculated spectra of  $^{138}\text{Te}$  and the consideration of the  $R_4 = (E(4_1^+)/E(2_1^+))$  value, the spectrum appears to be vibrational. But closer inspection reveals that the spacing between yrast levels ( $E_{I+2} - E_I$ ) increases, although not exactly proportional to  $I$  (or from the plot of  $E_I$  vs  $I(I+1)$  (not shown)). Thus  $^{138}\text{Te}$  is not a strongly deformed nucleus but lies in the transitional region between spherical  $^{136}\text{Te}$  and prolate deformed  $^{139,140}\text{Te}$  [21, 33]. It is interesting to mention here that the  $^{137}\text{Te}$  spectrum shows a kind of regularity [20], and the spectrum of  $^{139}\text{I}$  was interpreted as characteristic of a spherical vibrator resulting from a weak interaction of the  $^{138}\text{Te}$  core with the odd proton. We may thus term the spectrum of  $^{138}\text{Te}$  as almost vibrational. Spectrum of  $^{138}\text{Xe}$  is similar to  $^{138}\text{Te}$  but the regularity mentioned for  $^{138}\text{Te}$  is not clearly present in  $^{138}\text{Xe}$ . However from the consideration of the spectrum in  $^{139}\text{Xe}$  [34] and our recent work [25], we may also term the spectrum of  $^{138}\text{Xe}$  as almost vibrational. For  $^{138}\text{Ba}$  (Fig.8), predictions for the energy values of the level spectra are also remarkably good, though the spacings between the  $2_2^+$ ,  $6_2^+$  and  $2_3^+$  levels are not very accurately reproduced. But it is remarkable that for  $^{138}\text{Sn}$ , where experimental level scheme is not known, the two results differ dramatically (Fig.5). The first three excited states  $2^+$ ,  $4^+$ ,  $6^+$ , as discussed in section A, appear at about double excitation energies in the calculation with the CWG Hamiltonian. There is a large energy gap  $\simeq 2$  MeV between the  $6_1^+$  and  $8_1^+$  states for SMPN

calculation. But this gap is only about 0.8 MeV for CWG results. This energy gap of about 0.6-0.8 MeV between  $6_1^+$  and  $8_1^+$  states also exists in the experimental as well as calculated spectra of  $^{138}\text{Te}$ ,  $\text{Xe}$  for both the interactions. In the calculated spectrum of  $^{138}\text{Ba}$ , for both the interactions, this gap is  $\approx 1.1\text{MeV}$ . Thus the large gap between these states appears only with the SMPN Hamiltonian for  $^{138}\text{Sn}$ . These gaps primarily indicate that the states below and above these gaps necessarily belong to different multiplets. Each state belong predominantly to a particular muliplet. This can be understood well by viewing the occupancy plots in Figs. 9-12. For example, in  $^{138}\text{Sn}$ ,  $\nu 2f_{7/2}^6$  configuration can couple to  $J_{max} = 6$ . Thus for generating the  $8^+$  state a pair of neutrons must be promoted to a higher lying single particle orbital creating the energy gap. This gap for the collective almost vibrational nuclei  $^{138}\text{Te}$ ,  $\text{Xe}$  also indicates the dominance of multiplets in the compositions of the wave functions of these vibrational states. At higher spins the agreement between two calculations improves.

## 2. Binding energies

The ground state binding energies and spin parities are important observables particularly for application in the nucleosynthesis calculation. Comparison of binding energies calculated for these nuclei using two interactions are shown in the Table IV. The SMPN results show good agreement with experimental data [35] for Te, Xe and Ba isotopes. The CWG results consistently show over binding for these nuclei, particularly with increasing proton numbers. But for Sn isotope, the SMPN shows some over binding. This was also noted in our previous work [10], where we have suggested a systematic correction for neutron - rich species. After introducing that correction for the Sn isotopes using the binding energy of  $^{136}\text{Sn}$  from SMPN, the results for  $^{138}\text{Sn}$  matches with those from CWG. The experimental binding energy value for  $^{138}\text{Sn}$  is still not available. The binding energies for  $^{136}\text{Sn}$  and  $^{138}\text{Te}$  are obtained from systematics and therefore may have substantial errors. Moreover, it is important to note that CWG predicts a  $2^-$  ground state (B.E=- 55.503 MeV) instead of the observed  $3^-$  in  $^{138}_{55}\text{Cs}_{83}$ . SMPN correctly predicts [17] the ground state spin-parity in it with the binding energy value of -50.867 MeV, which compares very well with the measured value of -50.849(17) MeV [35]. The SMPN set of 2-body matrix elements can also reproduce rather well the  $6^-$  isomer in  $^{138}\text{Cs}$  [17]. Interestingly, no other interaction that we have used, *viz.*, KH5082, CW5082,

TABLE I: Energy (MeV) spectra and wave functions of yrast levels of  $^{138}\text{Sn}$  in full and truncated spaces using SMPN interaction. The dominant particle - partitions are marked as A( $\nu 2f_{7/2}^6$ ), B ( $\nu 2f_{7/2}^5 1h_{9/2}$ ) and C ( $\nu 2f_{7/2}^5 3p_{3/2}$ ). The effect of the intruder state  $1i_{13/2}$  is denoted by D ( $\nu 2f_{7/2}^4 1i_{13/2}^2$ ). The B(E2) values are calculated for 0.64e value of neutron effective charge.

$I^\pi$	Full space		Truncated space	
	Energy	Wavefun.	Energy	Wavefun.
$0^+$	0.0	61% A (-20.184)	0.0	76% A (-19.571)
$2^+$	0.433	73%A, 3%D	0.135	81%A
$4^+$	0.738	79%A, 3%D	0.407	86%A
$6^+$	0.890	80%A, 3%D	0.551	86%A
$8^+$	2.825	64%B, 4%D	2.449	77%C
$10^+$	3.195	77%B, 2%D	2.767	81%B
B(E2, $0_{gs}^+ \rightarrow 2_1^+$ )		344.7	313.9	
		$e^2 fm^4$		

CWG .. etc., usually used in this valence space, can reproduce the isomeric nature of the  $6^-$  level with a half life of  $\approx 3$  minutes and even the  $3^-$  ground state is not reproduced in some of these calculations.

For CWG, this deficiency for nuclei with more valence protons than neutrons, can perhaps be attributed to the over binding of some of the most important  $\pi - \pi$  tbmes (to be discussed in Section III). Similarly, in SMPN, some important diagonal  $\nu - \nu$  tbmes still show slight over binding. Better prediction by SMPN is definitely due to the fact that at least some of its important tbmes contain empirical information appropriate to this exotic neutron-rich locality. We shall discuss it further in a following section.

### 3. Wave functions and B(E2) values

The structure of the wave functions of different spin states for the four isobars are compared in Table V and Figs (9-14). These results are obtained using both the SMPN and

TABLE II: Comparison of energies (MeV) and wavefunctions of  $0^+$  and  $2^+$  states of  $^{134,136,138}\text{Sn}$  using SMPN and CWG interactions. The contributions from the dominant  $2f_{7/2}$  multiplet ( $\nu 2f_{7/2}^n$ ) configurations are shown, where  $n$  is 2,4 and 6 for  $^{134,136,138}\text{Sn}$ , respectively. The B(E2) values are calculated for 0.64e value of neutron effective charge. The experimental  $2^+$  energy for  $^{134}\text{Sn}$  is 726 keV and  $B(E2, 0_{gs}^+ \rightarrow 2_1^+)$  is  $\simeq 295 e^2 fm^4$  [36].

$I^\pi$	SMPN [7]		Other [14]	
	Energy	Wavefun.	Energy	Wavefun.
$^{134}\text{Sn}$				
$0^+$	0.0 (fitted)	65%	0.0	78%
	(-6.363)		(-6.221)	
$2^+$	0.733 (fitted)	79%	0.774	78%
	$R_4 = E_{4_1^+}/E_{2_1^+}$	1.46		1.44
	$B(E2, 0_{gs}^+ \rightarrow 2_1^+)$	289.2		307.8
	$(e^2 fm^4)$	(1.42 W.u.)		(1.51 W.u.)
$^{136}\text{Sn}$				
$0^+$	0.0	56%	0.0	54%
	(-13.041)		(-12.497)	
$2^+$	0.578	68%	0.733	49%
	$R_4 = E_{4_1^+}/E_{2_1^+}$	1.53		1.58
	$B(E2, 0_{gs}^+ \rightarrow 2_1^+)$	449.0		623.5
	$(e^2 fm^4)$	(2.16 W.u.)		(3.0 W.u.)
$^{138}\text{Sn}$				
$0^+$	0.0	61%	0.0	32%
	(-20.184)		(-18.737)	
$2^+$	0.433	73%	0.761	24%
	$R_4 = E_{4_1^+}/E_{2_1^+}$	1.70		1.78
	$B(E2, 0_{gs}^+ \rightarrow 2_1^+)$	344.7		916.8
	$(e^2 fm^4)$	(1.63 W.u.)		(4.33 W.u.)

TABLE III: Dimensions of matrices involved in different isotopes for different yrast states.

$I^\pi$	$^{138}\text{Sn}$	$^{138}\text{Te}$	$^{138}\text{Xe}$	$^{138}\text{Ba}$
$0^+$	2411	22960	13416	518
$2^+$	10713	105489	60955	2134
$4^+$	16321	160243	90982	3053
$6^+$	18351	179054	99241	3170
$8^+$	17271	167325	90114	2715
$10^+$	14284	137121	71324	2000

TABLE IV: The binding energy (MeV) results for different A=138 isobars with SMPN and CWG. The experimental values are also shown. Experimental errors are shown within parentheses.

Nucleus	Other [14]		
	Binding Energy (MeV)		
	Expt.	Theoretical	
		SMPN	CWG
$^{138}\text{Sn}$	-	-20.184	-18.737
	-	-18.56 <sup>a</sup>	
$^{138}\text{Te}$	-36.24(21)	-37.303	-37.692
	-	-36.60 <sup>a</sup>	
$^{138}\text{Xe}$	-48.89( 4)	-49.011	-51.906
$^{138}\text{Ba}$	-55.44( 1)	-55.266	-62.096

<sup>a</sup> The binding energy values after systematic corrections done according to Ref. [10]

CWG interaction. The extent of configuration mixing involved in each yrast state up to  $10^+$  for these isotopes are compared in Table V. We have tabulated (i)  $S$ , the sum of contributions from particle partitions each of which is contributing greater than 1.00%, (ii)  $M$ , maximum contribution from a single partition, (iii)  $N$ , total number of partitions contributing to  $S$ . Larger extent of configuration mixing usually leads to larger deviation of  $S$  from 100%. Similarly as mixing increases,  $M$ , i.e., the maximum contribution from a single partition gradually decreases. Increase in  $N$  also indicates larger mixing. From the table it can be found that CWG predicts more configuration mixed structure for the states in A=138 isobars compared to that predicted by SMPN. Figs. 9-12 show the occupancy plots

TABLE V: The extent of configuration mixing involved in different isotopes for different states. For each state the numbers in the parenthesis are (i)  $S$ , sum of contributions from particle partitions each of which is contributing greater than 1.00%, (ii)  $M$ , maximum contribution from a single partition, (iii)  $N$ , total number of partitions contributing in  $S$ .

$I^\pi$	$^{138}_{50}\text{Sn}_{88}$	$^{138}_{52}\text{Te}_{86}$	$^{138}_{54}\text{Xe}_{84}$	$^{138}_{56}\text{Ba}_{82}$
	$S, M, N$	$S, M, N$	$S, M, N$	$S, M, N$
SMPN				
$0^+$	90.7, 60.9, 6	69.5, 29.0, 15	72.5, 19.7, 19	93.3, 37.6, 10
$2^+$	92.4, 73.0, 6	64.7, 27.1, 15	65.2, 17.0, 15	90.7, 38.0, 13
$4^+$	93.8, 78.7, 6	69.6, 29.0, 18	68.1, 17.8, 16	91.1, 23.2, 14
$6^+$	95.8, 80.0, 7	71.0, 34.1, 15	76.1, 24.8, 16	94.8, 37.0, 13
$8^+$	93.0, 64.0, 9	70.4, 27.2, 15	69.9, 14.8, 19	95.3, 31.5, 10
$10^+$	94.8, 77.3, 7	73.5, 27.7, 11	75.9, 32.2, 16	98.0, 50.0, 9
CWG				
$0^+$	89.1, 31.9, 12	46.2, 11.3, 16	61.3, 19.3, 16	96.5, 35.1, 11
$2^+$	85.5, 23.9, 17	36.7, 6.4, 17	59.8, 13.3, 19	89.8, 40.6, 13
$4^+$	86.8, 42.9, 12	33.9, 5.0, 17	60.8, 12.8, 21	92.0, 35.3, 12
$6^+$	91.3, 54.9, 9	42.5, 6.2, 23	60.1, 14.8, 19	92.4, 41.0, 9
$8^+$	89.7, 43.9, 12	45.3, 6.1, 26	57.5, 8.9, 18	94.3, 45.7, 9
$10^+$	92.1, 44.0, 12	62.1, 9.3, 24	69.9, 15.7, 21	95.9, 43.2, 7

for yrast states in each of these nuclei with both interactions. As the figures show, multiplet structure with  $\nu 2f_{7/2}^6$  is more clear in SMPN results (Fig.9) for  $0^+$  to  $6^+$  state in  $^{138}\text{Sn}$ . In Fig.9, with CWG, increase in contributions from  $\nu 3p_{3/2}$ ,  $\nu 2f_{5/2}$  and  $\nu 1h_{9/2}$  orbitals is observed. For Te, although the mixing increases compared to Sn with SMPN, CWG still show larger extent of mixing. Similar result is obtained for  $^{138}\text{Xe}$ . The B(E2) peaks at Xe in both SMPN and CWG results (Table VI). Interestingly, for Ba, the two interactions give, except for the binding energy, more or less the same results both with respect to the energy spectrum (Fig. 8) as well as the wave functions and B(E2) values (Table V,VI and Figs. 13,14). The experimental B(E2,  $2_1^+ \rightarrow 0_{gs}^+$ ) for Ba [30] is 460 (18)  $e^2 fm^4$  compares well with 531  $e^2 fm^4$  from SMPN and 504  $e^2 fm^4$  for CWG. The effective charges used are

TABLE VI: The  $B(E2, 2_1^+ \rightarrow 0_{gs}^+)$  in  $e^2 fm^4$  for different A=138 isobars. The values in Weisskopf units are also shown within parentheses.

Interactions	$^{138}Sn$	$^{138}Te$	$^{138}Xe$	$^{138}Ba$
	$T_z=+3$	$T_z=+1$	$T_z=-1$	$T_z=-3$
SMPN	68.9(1.6)	484.6(11.5)	638.7(15.1)	530.6(12.5)
CWG	183.4(4.3)	737.8(17.4)	785.1(18.6)	504.4(11.9)

the standard ones,  $1.47e$  for protons and  $0.64 e$  for neutrons. It can be noted that proton effective charges,  $1.37e$  and  $1.41e$ , fit the  $B(E2, 2_1^+ \rightarrow 0_{gs}^+)$  in  $^{138}Ba$  with SMPN and CWG interactions, respectively. This value is  $\simeq 11$  W.u., a limiting value for vibrational collectivity. Although, the  $B(E2)$  value for  $^{138}Ba$  is in the range of vibrational collective excitations and the extent of configuration mixing is much larger than that in  $^{138}Sn$ , however, considering the overall feature of the spectrum, occupancy plots (Fig.12), the wave function structure (Table V, Fig. 13) and the  $R_4$  value of 1.4, it is reasonable to conclude that the excitations are of single particle nature. This means N=82 shell closure still prevails in a strong way with increasing proton number, but the  $Z = 50$  shell closure appears to be much weaker with the same number of valence neutrons. It is indeed satisfactory to note that the vibrational structure in  $^{138}Te, Xe$  is excellently reproduced in the shell model calculations. In order to show explicitly the amount of configurations contributing less than 1% in building the yrast states in these A=138 isobars, we compare in Figs. 13,14, the wave functions of the  $0_1^+$  states of  $^{138}Sn, Ba$  and  $^{138}Te, Xe$ . From these  $\pi$ -chart representations, it is easy to appreciate how vigorously fragmentation of parentages takes place as the states go from single particle to collective nature. The  $2_1^+$  states also show similar behaviour for all these isobars. The Figs. 9-12 show time averaged nucleon occupancies of the single particle states for the collective vibrational states in these nuclei. It can be noted that nucleons are excited to almost all of the single particle states (sps). For  $^{138}Te, Xe$ , any particular angular momentum state is generated by the contributions from all the various sps (Fig. 14). But, for  $^{138}Sn$ , (Fig.9) the occupancy plots clearly show the dominance of the contribution from a single orbital, namely,  $\nu 2f_{7/2}$  with both CWG and SMPN interactions.  $B(E2)$  values for  $^{138}Te, Xe$ , given in Table VI are in the range 15-20 W.u., consistent with the characterization of their spectra as vibrational.

So these comparisons clearly indicate that as far as the proton-proton two-body matrix elements are concerned, these two interactions have over all similar performances, except for the over binding of the  $\pi - \pi$  tbmes in CWG, affecting the binding energies (with respect to the  $^{132}\text{Sn}$  core) of the states. Moreover, it can be noted from Table VI, that the predicted  $B(E2, 2_1^+ \rightarrow 0_{gs}^+)$  values in  $^{138}\text{Sn}$ ,  $^{138}\text{Te}$  and  $^{138}\text{Xe}$  are somewhat larger with the CWG interaction.

### III. COMPARISON OF TBMES : EMPIRICAL AND REALISTIC INTERACTIONS

Spectroscopic data for very neutron-rich nuclei above the  $^{132}\text{Sn}$  core are being available recently. But available data are not sufficient yet to construct a fully empirical (1+2) body Hamiltonian. It is interesting to point out that the construction of empirical Hamiltonians for the n-rich environments in different mass regions might be important for checking the realistic interactions built from the fundamental bare N-N interaction. Comparison of the predictability of a realistic Hamiltonian over a model space, as well as its correlation with an empirical Hamiltonian with good predictive power over the same model space can help understanding how realistically various nucleon-nucleon correlations have been taken in to account in obtaining the realistic Hamiltonian.

For microscopic understanding of the available data on the structure of these very n-rich nuclei, one finds spherical shell model calculations very suitable for this region and thus needs appropriate nuclear Hamiltonian. Available KH5082 and CW5082 Hamiltonians and very recently effective interaction derived from CD-Bonn potential are being used. In our earlier work [7] we have shown that CW5082 Hamiltonian works reasonably well for  $N < 84$  isotones but fails for  $N \geq 84$  isotones.

Our work in Ref. [10], following the method of Chou and Warburton [37] is perhaps the first somewhat elaborate empirical approach to improve upon the existing Hamiltonian appropriate for this particular region. We used the available experimental data for the  $A=134$  Sn, Sb and Te nuclei available then. As mentioned above, our earlier studies showed that CW5082 is reasonable for  $N < 84$ . So we started with CW5082 and modified it as far as practicable with the limited experimental data available at that point of time. The motivation for these changes was also clearly stated in Ref. [10]. All the single particle energies (spes)

of the valence orbitals in the CW5082 were replaced by experimentally determined ones, except the  $\pi 3s_{1/2}$  and  $\nu 1i_{13/2}$  spes (Table VII). These two spes were obtained as stated in Ref. [10]. Out of 2101 two-body matrix elements, 26 tbmes of CW5082 interaction were changed using the data on the binding energies of the ground states and low-lying spectra of the A=134 isobars of Sn, Sb and Te nuclei only and not any other nuclei above the core. It should be noted that these A=134 nuclei provide information on the neutron-neutron ( $\nu - \nu$ ), proton-neutron ( $\pi - \nu$ ) and proton-proton ( $\pi - \pi$ ) tbmes, respectively. Modified CW5082 was named as SMPN and have been used for shell model calculations for almost all neutron-rich nuclei above  $^{132}\text{Sn}$  core in the range  $134 \leq A \leq 138$ . Some of the results have been presented in [10, 15, 16, 17]. It should be mentioned that the new interaction predict better results, compared to CW5082 and other interactions being used in this region, for N<84 nuclei too. The relevant spes and tbmes of CW5082, CWG [14] and SMPN are compared in Tables VII and VIII, respectively.

It was already pointed out by Chou and Warburton [37] that a glaring deficiency in Kuo-Herling interaction, which is the basic ingredient of CW5082, is that the neutron-neutron J=0 tbmes are too attractive. So for an approximate adjustment of this defect those tbmes were multiplied by 0.6 in KH5082 and CW5082 [37]. Six diagonal  $\nu - \nu$  tbmes with  $(J^\pi, T) = (0^+, 1)$  of SMPN are further reduced by about 50% compared to those of CW5082. The reduction of these tbmes, the so-called pairing terms were obtained [8, 10] by adjusting them to reproduce the binding energy of  $^{134}\text{Sn}$ . Corresponding tbmes of CWG are relatively overbound.

The neutron-neutron J=0 tbmes, the pairing terms, are indeed different from those expected from standard pairing interaction. But in view of the consistently improved predictability of SMPN for the binding energies, level spectra and other spectroscopic properties for almost all the n-rich nuclei in the range  $134 \leq A \leq 138$  as delineated in the present work and elsewhere [10, 15, 16, 17], it may be reasonable to conclude that the  $\nu - \nu$  pairing terms are indeed reduced in this neutron -rich environment. Moreover, slight over binding of the ground states of Sn isotopes above  $^{132}\text{Sn}$  as obtained with the SMPN Hamiltonian suggests further reduction of these matrix elements, which may be due to increasing A or uncertainties in some of the spes. This reduction of the  $\nu - \nu$  pairing terms observed [8, 10] from the shell model applications is consistent with the recent observations [4, 5].

Three other modified diagonal  $\nu - \nu$  tbmes with  $(J^\pi, T) = (2^+, 4^+, 6^+, 1)$  are also given in

TABLE VII: Single particle energies used in SMPN [10], CWG [14] and CW5082 [37] Hamiltonians.

State	Energy (MeV)			State	Energy (MeV)		
	SMPN	CWG	CW5082		SMPN	CWG	CW5082
$\pi 1g_{7/2}$	-9.66290	-9.66300	-9.59581	$\nu 1h_{9/2}$	-0.89400	-0.89440	-0.89500
$\pi 2d_{5/2}$	-8.70000	-8.70050	-8.67553	$\nu 2f_{7/2}$	-2.45500	-2.45530	-2.38000
$\pi 2d_{3/2}$	-7.22300	-7.22328	-6.95519	$\nu 2f_{5/2}$	-0.45000	-0.45070	-0.89000
$\pi 3s_{1/2}$	-7.32300	-6.96570	-6.92783	$\nu 3p_{3/2}$	-1.60100	-1.60160	-1.62500
$\pi 1h_{11/2}$	-6.87000	-6.87141	-6.83792	$\nu 3p_{1/2}$	-0.79900	-0.79960	-1.16000
				$\nu 1i_{13/2}$	0.25000	0.239700	-0.29000

the table. Tbmcs  $\langle 2f_{7/2}^2 | V | 2f_{7/2}^2 \rangle^{J=2,4}$  have the same phases for all the three interactions, but their magnitudes in SMPN are larger than the corresponding values in CW5082 and CWG. This is because we have assumed purer multiplet structure for  $2^+$  to  $6^+$  and also for  $8^+$  of  $^{134}\text{Sn}$ , while adjusting the tbmes to reproduce the experimental level scheme. Diagonal  $\langle 2f_{7/2}^2 | V | 2f_{7/2}^2 \rangle^{J=6}$  of SMPN is out of phase with that of CW5082 and CWG. The other modified  $\nu - \nu$  tbme  $\langle 1h_{9/2}^2 2f_{7/2} | V | 1h_{9/2}^2 2f_{7/2} \rangle^{J=8}$  also has somewhat larger value in SMPN.

Proton - proton diagonal tbmes of the CWG with  $J=0,2,4$  show overbinding compared to other two interactions. The CWG tbme with  $J=6$  has much smaller magnitude compared to that for the other two interactions. Comparison of the binding energies and spectra for  $^{138}\text{Te}$ ,  $^{138}\text{Xe}$  and  $^{138}\text{Ba}$  clearly suggests that these most important  $\pi - \pi$  tbmes are indeed overbound in case of the CWG interaction.

All the neutron-proton ( $\pi - \nu$ ) tbmes in the  $T=0$  channel given in the table have the same phases in these three interactions. But the  $\pi - \nu$  tbmes of the SMPN interaction are found to be stronger.

#### IV. SUMMARY AND CONCLUSIONS

The neutron- rich  $^{132}\text{Sn}$  region is an interesting domain to study the N-N interaction in the neutron-rich environment. Our comparison of the calculated results for the  $E_{2_1^+}$ ,  $E_{4_1^+}$  and  $E_{6_1^+}$  level energies with the local systematic trends reveal the evolution of the shell structure below and above the  $Z = 50$ ,  $N = 82$  shell closure. Both the interactions, SMPN and CWG are quite capable of reproducing the existing experimental data for  $A=138$  isobars, namely

TABLE VIII: The relevant tbmes of CW5082 [37], CWG [14] and SMPN [10] have been compared. The valence orbitals have been enumerated according to the following convention: PROTONS :  $1g_{7/2}(1)$ ,  $2d_{5/2}(2)$ ,  $2d_{3/2}(3)$ ,  $3s_{1/2}(4)$ ,  $1h_{11/2}(5)$ ; NEUTRONS:  $1h_{9/2}(6)$ ,  $2f_{7/2}(7)$ ,  $2f_{5/2}(8)$ ,  $3p_{3/2}(9)$ ,  $3p_{1/2}(10)$ ,  $1i_{13/2}(11)$

Indices	J	T	Hamiltonians		
			CW5082	CWG	SMPN
n-p tbmes					
1 7 1 7 0 0			-0.6778	-0.7922	-0.7355
1 7 1 7 1 0			-0.336	-0.5390	-0.743
1 7 1 7 2 0			-0.29336119	-0.3739	-0.4067
1 7 1 7 3 0			-0.30348513	-0.2385	-0.354
1 7 1 7 4 0			-0.09123172	-0.1290	-0.227
1 7 1 7 7 0			-0.42997605	-0.5440	-0.535
1 6 1 6 8 0			-0.68749624	-0.9491	-1.037
1 11 1 11 10 0			-0.61499959	-0.7795	-0.764
5 7 5 7 9 0			-0.57939130	-0.5890	-1.058
5 11 5 11 10 0			-0.08622793	-0.2972	-1.942
5 11 5 11 11 0			-0.12218534	-0.0354	-1.611
5 11 5 11 12 0			-0.75382543	-1.1495	-1.519
p-p tbmes					
1 1 1 1 0 1			-0.66390	-0.9972	-0.56100
1 1 1 1 2 1			0.16450	-0.2838	0.2050
1 1 1 1 4 1			0.38240	-0.0257	0.5682
1 1 1 1 6 1			0.43640	0.1008	0.5120
n-n tbmes: pairing terms					
6 6 6 6 0 1			-0.61197406	-1.2944	-0.293747544
7 7 7 7 0 1			-0.48571584	-0.6718	-0.233143598
8 8 8 8 0 1			-0.27602252	-0.4515	-0.132490814
9 9 9 9 0 1			-0.37947276	-0.5884	-0.182146922
10 10 10 10 0 1			-0.10030835	-0.1606	-0.0481480062
11 11 11 11 0 1			-0.70925683	-0.9751	-0.340443283
n-n tbmes					
7 7 7 7 2 1			-0.31314358	-0.2983	-0.453
7 7 7 7 4 1			-0.05632162	-0.0909	-0.29
7 7 7 7 6 1			0.05457612	0.0011	-0.162
6 7 6 7 8 1			-0.25914928	-0.3974	-0.495

$^{138}\text{Te}$ ,  $^{138}\text{Xe}$  and  $^{138}\text{Ba}$ . But the predicted spectra for  $^{138}\text{Sn}$  using these two interactions differ significantly. The SMPN results fit nicely to the systematics of the nuclei ( $Z=52-60$ ) above  $^{132}\text{Sn}$  core. For neutron number  $< 82$ , the  $\text{Sn}$  ( $Z=50$ ) isotopes have a special status due to its semi- shell closed structure. But for increasing neutron number ( $> 82$ ), the  $Z=50$  shell closure weakens and  $\text{Sn}$  isotopes behave very similar to the other  $Z=52-60$  nuclei. But with CWG, the weakening is not much dramatic,  $\text{Sn}$  isotopes ( $N=86,88$ ) still retain some speciality, although to a lesser extent. Which picture is correct and represent the real situation can only be resolved by experimental data. Comparing the structure of the states in  $^{138}\text{Ba}$  with six valence protons with that of the  $^{138}\text{Sn}$  with the same number of neutrons, it is found that the protons in this valence space are more efficient in generating configuration mixing. This is essentially due to close spacing between  $\pi(gds)$  single particle orbitals that permits  $\pi - \pi$  residual interaction to scatter easily protons to various single particle states. This comparison also indicates that the increasing neutron number weakens  $Z=50$  shell closure in a stronger way than an equal number of protons can do to the  $N=82$  shell closure.

The results for the spectra and binding energies of the ground states of  $^{138}\text{Te}$ ,  $^{138}\text{Xe}$  and  $^{138}\text{Ba}$ , when compared more precisely show that SMPN predictions are more close to the experimental data. This better predictability of the SMPN interaction over the CWG may be attributed to the fact that SMPN incorporates in some of its important tbmes, the special features of the N-N interaction in the exotic n-rich environment above the  $^{132}\text{Sn}$  core. This perhaps suggests for exotic n-rich environments in general, the essentiality of incorporation of the local spectroscopic information in obtaining tbmes of the shell model Hamiltonian for better predictability towards dripline.

Our results using SMPN interaction clearly rule out the possibility of onset of collectivity in the low-lying yrast states of even  $\text{Sn}$  isotopes around  $N=88$ , whereas the results with the CWG interaction possibly shows an indication of gradual onset of collectivity. However, both the interactions reproduce remarkably well the collective vibrational spectra in  $^{138}\text{Te}, \text{Xe}$ , with the equal number of np-pairs. For nuclei with more than one neutron and proton in the valence space, mild deformation appears even before  $N=87$ , at  $N=84,85$  ( $^{137}\text{I}$  and  $^{137}\text{Te}$ ) and deformation/collectivity grows with increasing  $N$  and  $Z$ . In SMPN, tbmes scaled from non exotic  $^{208}\text{Pb}$  region have been changed by using spectroscopic information of  $A = 134$  isobars of  $\text{Sn}, \text{Sb}$  and  $\text{Te}$  only. Particularly, the diagonal  $J=0$  n-n tbmes, the so called pairing

terms, had to be reduced by a factor of 0.288. In CWG too, n-n times have been reduced. These reduction of n-n pairing interaction is consistent with other recent results as discussed above and seems to be generic for exotic n- rich environments. Comparison of the times of the three interactions enhances the belief that the N-N interaction is indeed different in nuclei in the very n-rich environment than that near the line of stability.

## V. ACKNOWLEDGMENTS

The authors thank Prof. Waldek Urban for many stimulating discussions on the issues in this mass region. Special thanks are due to Prof. B.A. Brown for his help in providing us his OXBASH (Windows Version) and the Nushell@MSU code.

- 
- [1] J.P. Schiffer et al., Phys. Rev. Lett. **92**, 162501 (2004).
  - [2] J. Shergur *et al.*, Phys. Rev. C **72**,024305 (2005), J. Shergur *et al.*, Phys. Rev. C **65**,034313 (2002); J. Shergur *et al.*, Nucl. Phys. A **682**, 493c (2001).
  - [3] D.C. Radford *et al.*, Phys. Rev. Lett. **88**, 222501 (2002).
  - [4] Rituparna Kanungo, Nucl. Phys. A **722**, 30c (2003).
  - [5] J. Terasaki, J. Engel, W. Nazarewicz, M. Stoitsov, Phys. Rev. C **66**, 054313 (2002).
  - [6] A. Wöhr *et al.*, Third Int. Conf. on Fission and Properties of Neutron-Rich Nuclei, November 3 - 9, 2002, Sanibel Island, Florida.
  - [7] Sukhendusekhar Sarkar, M. Saha Sarkar, Phys. Rev. C **64**, 014312 (2001)and references therein.
  - [8] Sukhendusekhar Sarkar, Proc. DAE-BRNS Symp. Nucl. Phys. (India) A **45**, 72 (2002).
  - [9] D.J. Dean *et al.*, Prog. Part. Nucl. Phys. **53**, 419 (2004) and references therein.
  - [10] Sukhendusekhar Sarkar, M. Saha Sarkar, Eur. Phys. Jour. **A21**, 61 (2004) and references therein.
  - [11] S. Sarkar and M. Saha Sarkar, Proc. DAE-BRNS Symp. Nucl. Phys. (India) **47** B, 58 (2004);
  - [12] Sukhendusekhar Sarkar and M. Saha Sarkar, Proc. 4th International Balkan School on Nuclear Physics, Bodrum, Turkey, 22-29 September 2004: Balkan Phys. Letts. Special Is-

- sue, 2004, Pg, 308; <http://arxiv.org/abs/nucl-th/0503067>; S. Sarkar and M. Saha Sarkar, <http://arxiv.org/abs/nucl-th/0507034>, Proc.of International Workshop on "Nuclear Structure Physics at the Extremes: New Directions" (NUSPE'05), 21-24 March, 2005, Shimla India; Sukhendusekhar Sarkar, W. Urban, M. Saha Sarkar, Proc. DAE-BRNS Symp. Nucl. Phys. (India) 50 (2005) 256;;
- [13] L. Coraggio, A. Covello, A. Gargano, and N. Itaco, Phys. Rev. C **72**, 057302 (2005) and references therein.
- [14] B.A. Brown, N. J. Stone, J. R. Stone, I. S. Towner, and M. Hjorth-Jensen, Phys. Rev. C **71**, 044317 (2005).
- [15] W. Urban, M. Saha Sarkar, S. Sarkar, T. Rzača-Urban, J.L. Durell, A.G. Smith, J.A. Genevey, J.A. Pinston, G.S. Simpson, I. Ahmad, Eur. Phys. J. A **27**, 257 (2006)(Letter).
- [16] T. Rzača-Urban, K. Pagowska, W. Urban, A. Zlomaniec, J. Genevey, J. A. Pinston, G. S. Simpson, M. Saha Sarkar, S. Sarkar, H. Faust, A. Scherillo, I. Tsekhanovich, R. Orlandi, J. L. Durell, A. G. Smith, and I. Ahmand, Phys. Rev. C **75**, 054319 (2007).
- [17] T. Rzača-Urban, W. Urban, M. Saha Sarkar, S. Sarkar, J.L. Durell, A.G. Smith, B.J. Varley, and I. Ahmad, Euro. Phys. Jour. A **32**, 5 (2007)(Letter); K.P. Kanta, S. Sarkar and M. Saha Sarkar, Proc. DAE-BRNS Symp. Nucl. Phys. (India) **47B**, 144 (2004).
- [18] M. P. Kartamyshev, T. Engeland, M. Hjorth-Jensen, and E. Osnes, Phys. Rev. C **76**, 024313 (2007) and references therein.
- [19] A. Korgul *et al.*, Eur. Phys. J. A **12**, 129 (2001).
- [20] W. Urban *et al.*, Phys. Rev. C **61**, 041301 (R) (2000).
- [21] F. Hoellinger *et al.*, Euro. Phys. Jour. A **6**, 375 (1999).
- [22] A. Korgul *et al.*, Eur. Phys. J. A **7**, 167 (2000).
- [23] W. Urban *et al.*, Phys. Rev. C **65**, 024307 (2002).
- [24] <http://www.nndc.bnl.gov>.
- [25] Ritesh Kshetri, M. Saha Sarkar, S. Sarkar, Phys. Rev. C **74**, 034314 (2006).
- [26] B.A. Brown *et al.*, Oxbash for Windows PC, MSU-NSCL Report No. **1289**, (2004).
- [27] S. Sarkar and M. Saha Sarkar, Proc. DAE-BRNS Symp. Nucl. Phys. (India) B **47**, 58 (2004).
- [28] Nushell@MSU, B. A. Brown and W. D. M. Rae, MSU-NSCL report (2007).
- [29] M. Saha Sarkar and S. Sarkar, Proc. DAE-BRNS Symp. Nucl. Phys. (India) **51**, 79 (2006).
- [30] S. Raman, C.W. Nestor, Jr., P. Tikkanen, At. Data Nucl. Data Tables **78**, 1 (2001).

- [31] I. Stefanescu *et al.*, Fourth Int. Conf. on Fission and Properties of Neutron-Rich Nuclei, November 11 - 17, 2007, Sanibel Island, Florida.
- [32] Sukhendusekhar Sarkar and Maitreyee Saha Sarkar, Fourth Int. Conf. on Fission and Properties of Neutron-Rich Nuclei, November 11 - 17, 2007, Sanibel Island, Florida.
- [33] W. Urban *et al.*, Phys. Rev. C **62**, 044315 (2000).
- [34] W. Urban *et al.*, Phys. Rev. C **66**, 044302 (2002).
- [35] G. Audi, A.H. Wapstra, and C. Thibault, Nucl. Phys. A **729**, 337 (2003).
- [36] R.L. Varner *et al.*, Eur. Phys. J. A **25**, s01, 391 (2005).
- [37] W.-T. Chou and E. K. Warburton, Phys. Rev. C **45**, 1720 (1992).

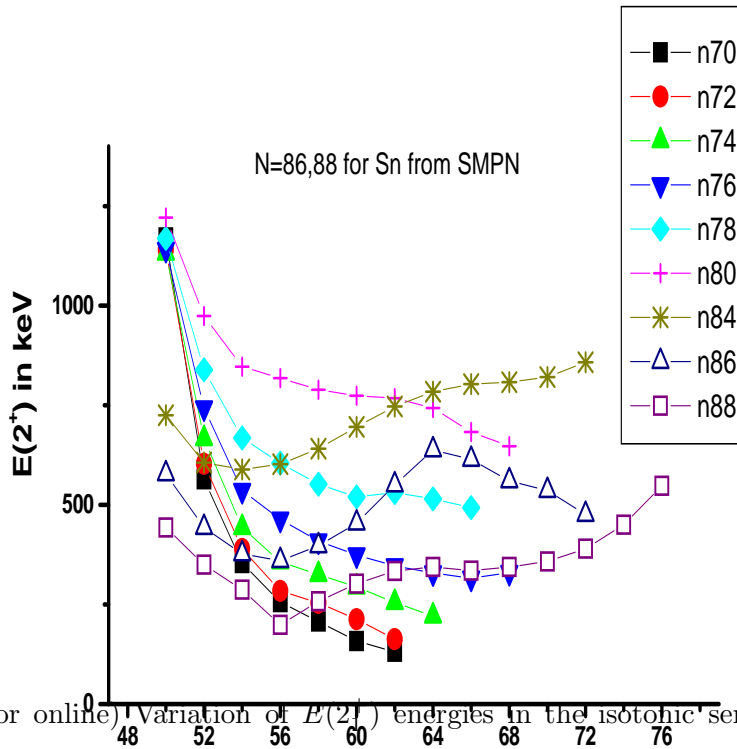


FIG. 1: (Color online) Variation of  $E(2^+)$  energies in the isotonic series. Predicted values for  $^{136,138}\text{Sn}$  using SMPN are shown in the figure. The other values are from experiments [24].

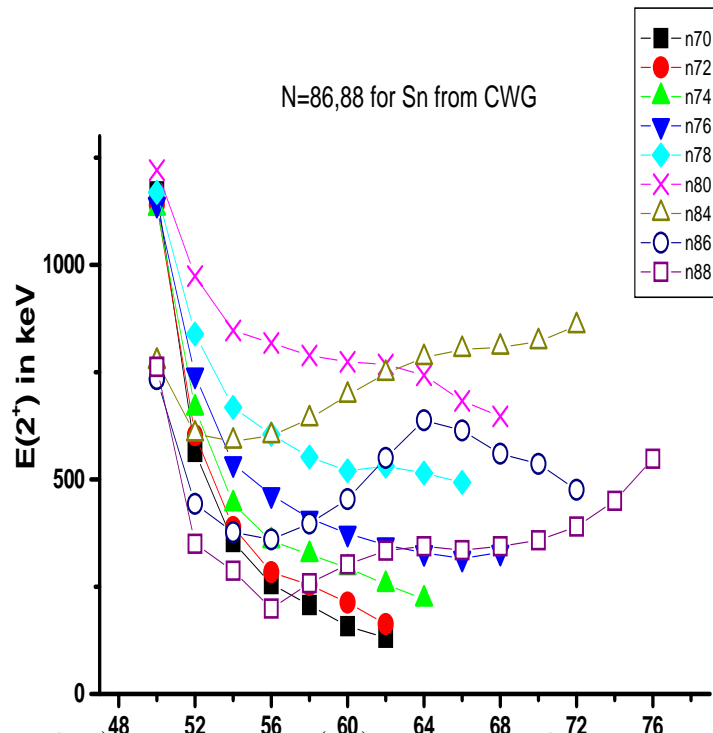


FIG. 2: (Color online) Variation of  $E(2_1^+)$  energies in the isotonic series. Predicted values for  $^{136,138}\text{Sn}$  using CWG are shown in the figure. The other values are from experiments [24].

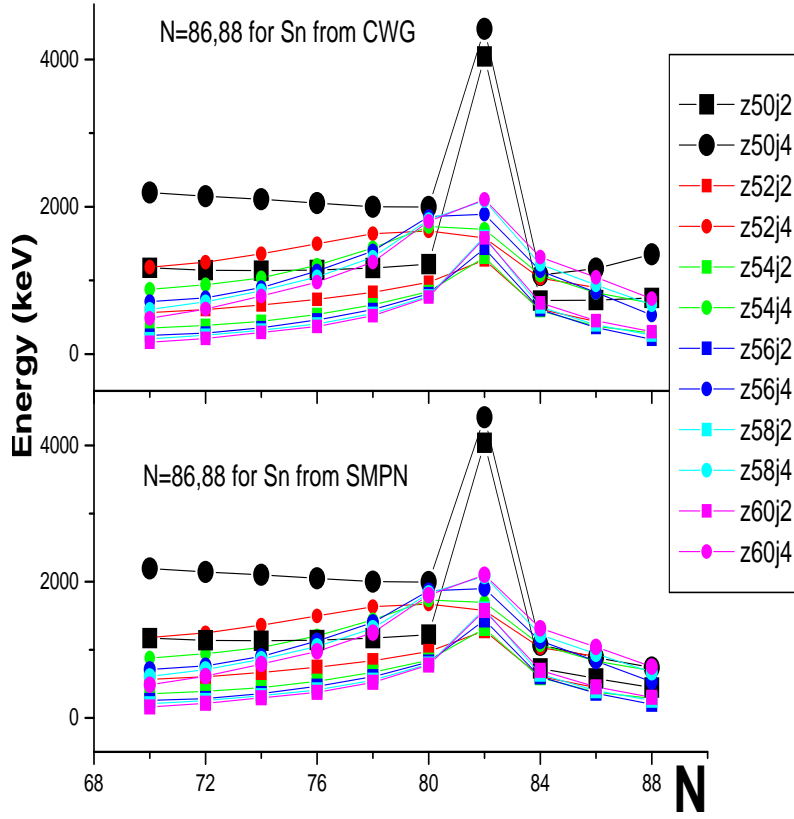


FIG. 3: (Color online) Variation of the ( $E(2_1^+)$  and  $E(4_1^+)$ ) of the isotopic series of  $Z=50$  to  $60$  with neutron numbers ranging from  $70$  to  $88$  is shown. Predicted values for  $^{136,138}\text{Sn}$  using CWG are shown in upper figure, while those using SMPN are in the lower one. The other values are from experiments [24].

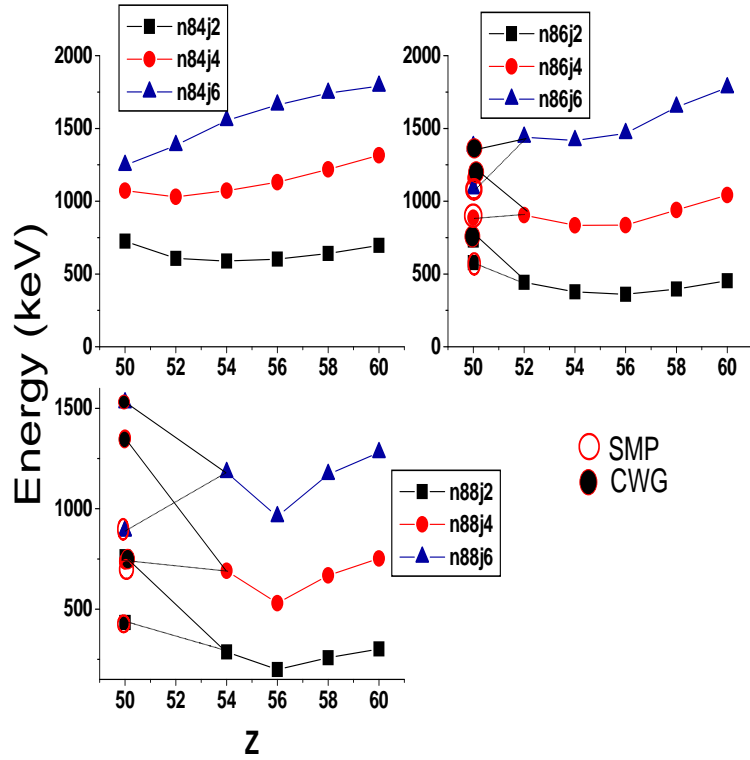


FIG. 4: (Color online) Variation of  $E(2_1^+)$ ,  $E(4_1^+)$  and  $E(6_1^+)$  for  $N=84$ ,  $86$  and  $88$  for  $Z=50-60$  is shown. The results from SMPN and CWG (for  $N=86,88$ ) are shown in the Figure. The other values are from experiments [24].

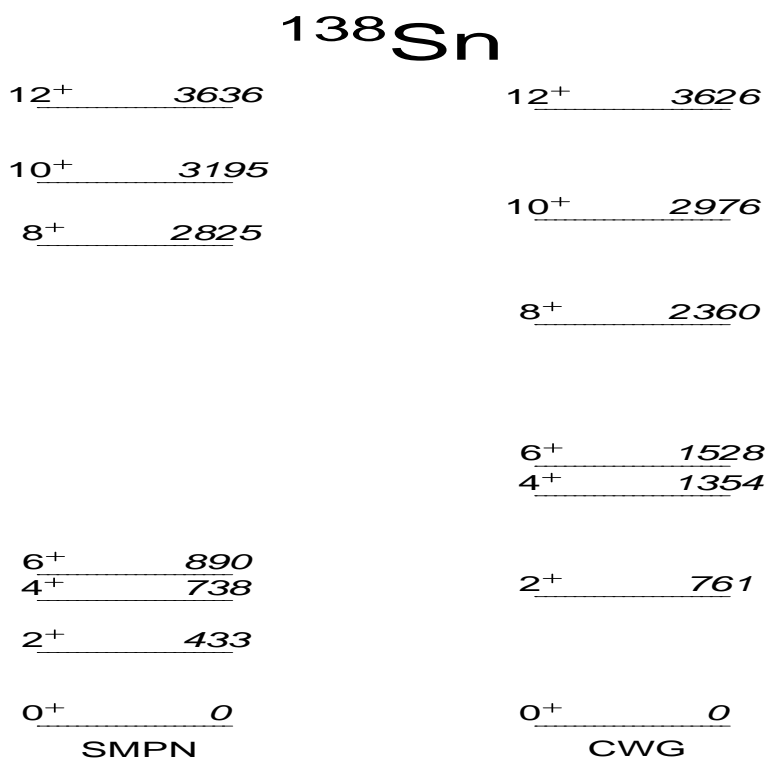


FIG. 5: The calculated excitation spectra using SMPN and CWG interactions.

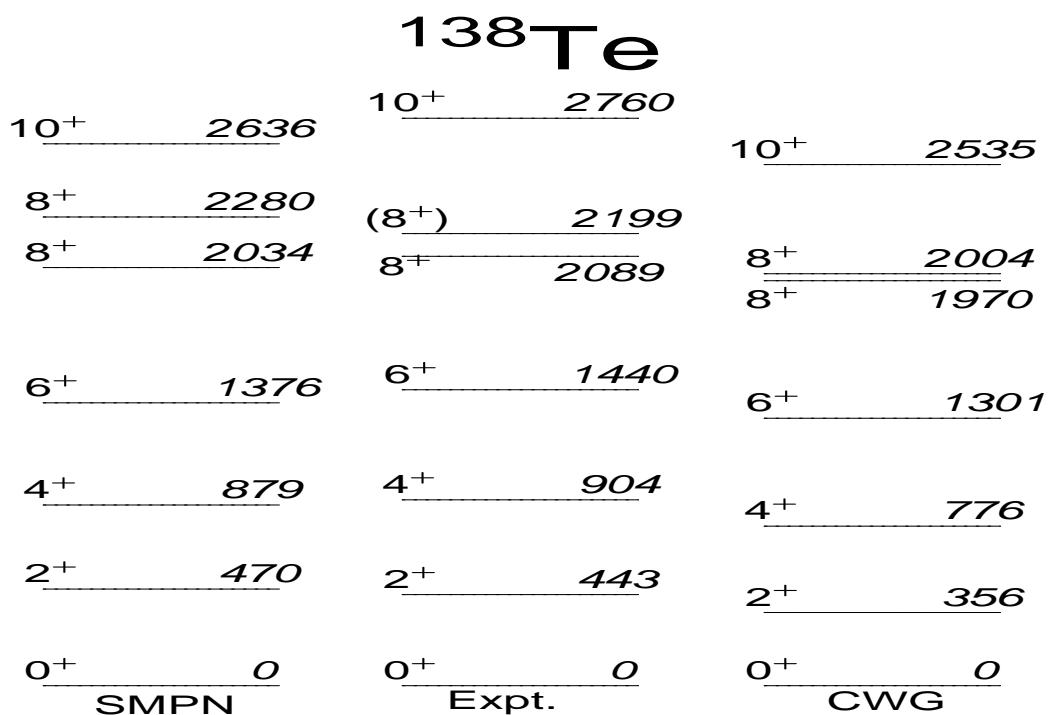


FIG. 6: Comparison of experimental and calculated excitation spectra using SMPN and CWG interactions.

# $^{138}\text{Xe}$

$10^+$ <u>2944</u>	$10^+$ <u>2972</u>	$10^+$ <u>2901</u>
$8^+$ <u>2260</u>	$8^+$ <u>2284</u>	$8^+$ <u>2171</u>
$6^+$ <u>1498</u>	$6^+$ <u>1555</u>	$6^+$ <u>1461</u>
$4^+$ <u>1077</u>	$4^+$ <u>1072</u>	$4^+$ <u>931</u>
$2^+$ <u>588</u>	$2^+$ <u>588</u>	$2^+$ <u>473</u>
$0^+$ <u>0</u>	$0^+$ <u>0</u>	$0^+$ <u>0</u>
SMPN	Expt.	CWG

FIG. 7: Same as Fig.6

# $^{138}\text{Ba}$

$10^+$ <u>3486</u>		$10^+$ <u>3691</u>
$8^+$ <u>3098</u>		$8^+$ <u>3251</u>
$6^+$ <u>2379</u>		$2^+$ <u>2458</u>
$2^+$ <u>2329</u>		$2^+$ <u>2292</u>
$2^+$ <u>2213</u>	$6^+$ <u>2217</u> $2203$	$6^+$ <u>2269</u>
$6^+$ <u>1957</u>	$6^+$ <u>2189</u>	$6^+$ <u>2071</u>
$4^+$ <u>1915</u>	$6^+$ <u>2090</u>	$4^+$ <u>1981</u>
	$4^+$ <u>1899</u>	$2^+$ <u>1477</u>
$2^+$ <u>1348</u>	$2^+$ <u>1436</u>	
$0^+$ <u>0</u>	$0^+$ <u>0</u>	$0^+$ <u>0</u>
SMPN	Expt.	CWG

FIG. 8: Same as Fig.6

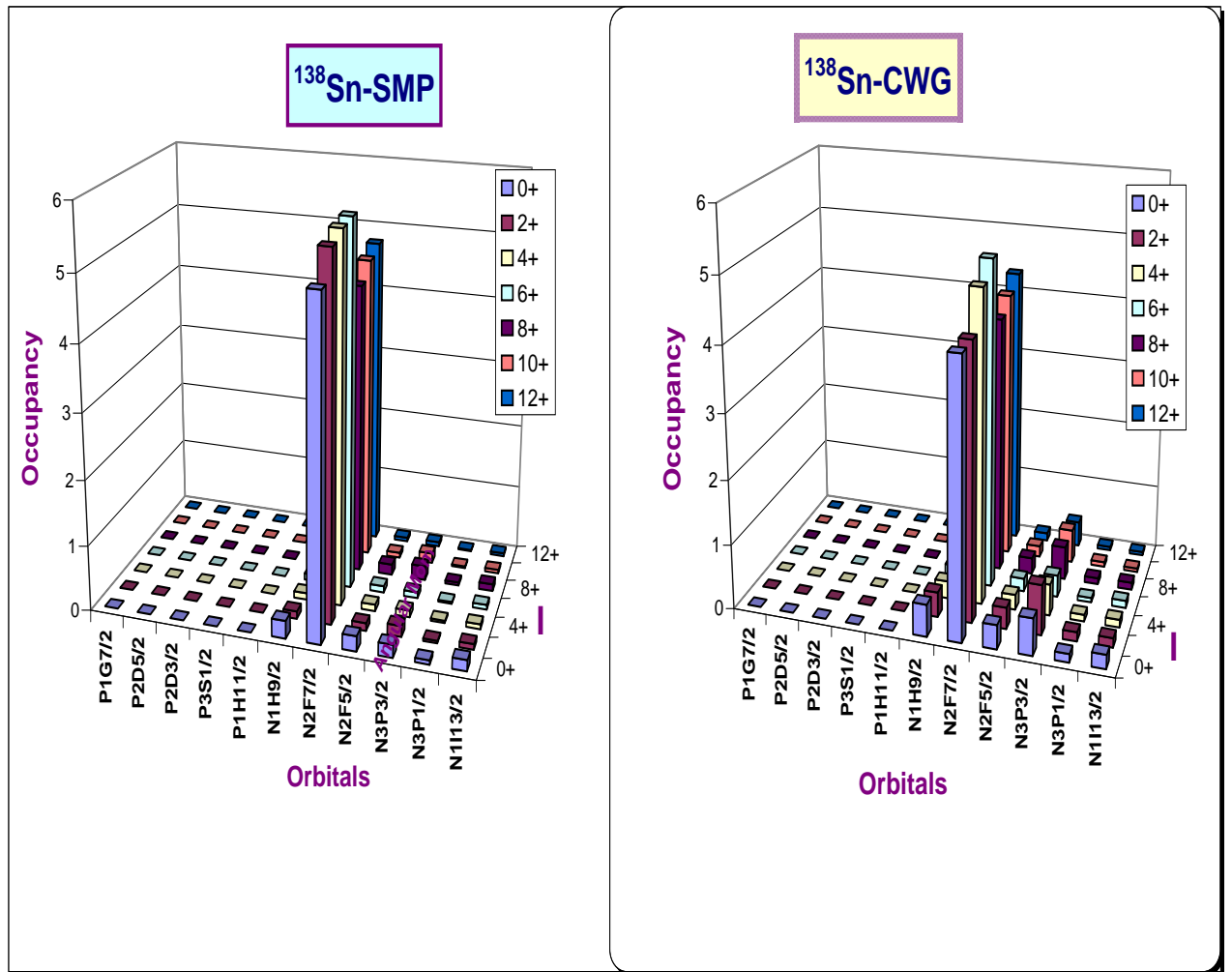


FIG. 9: (Color online) The number of neutrons occupying the orbitals indicated along the x-axis are plotted for different angular momentum states of this nucleus. The results using two interactions are indicated in the figure.

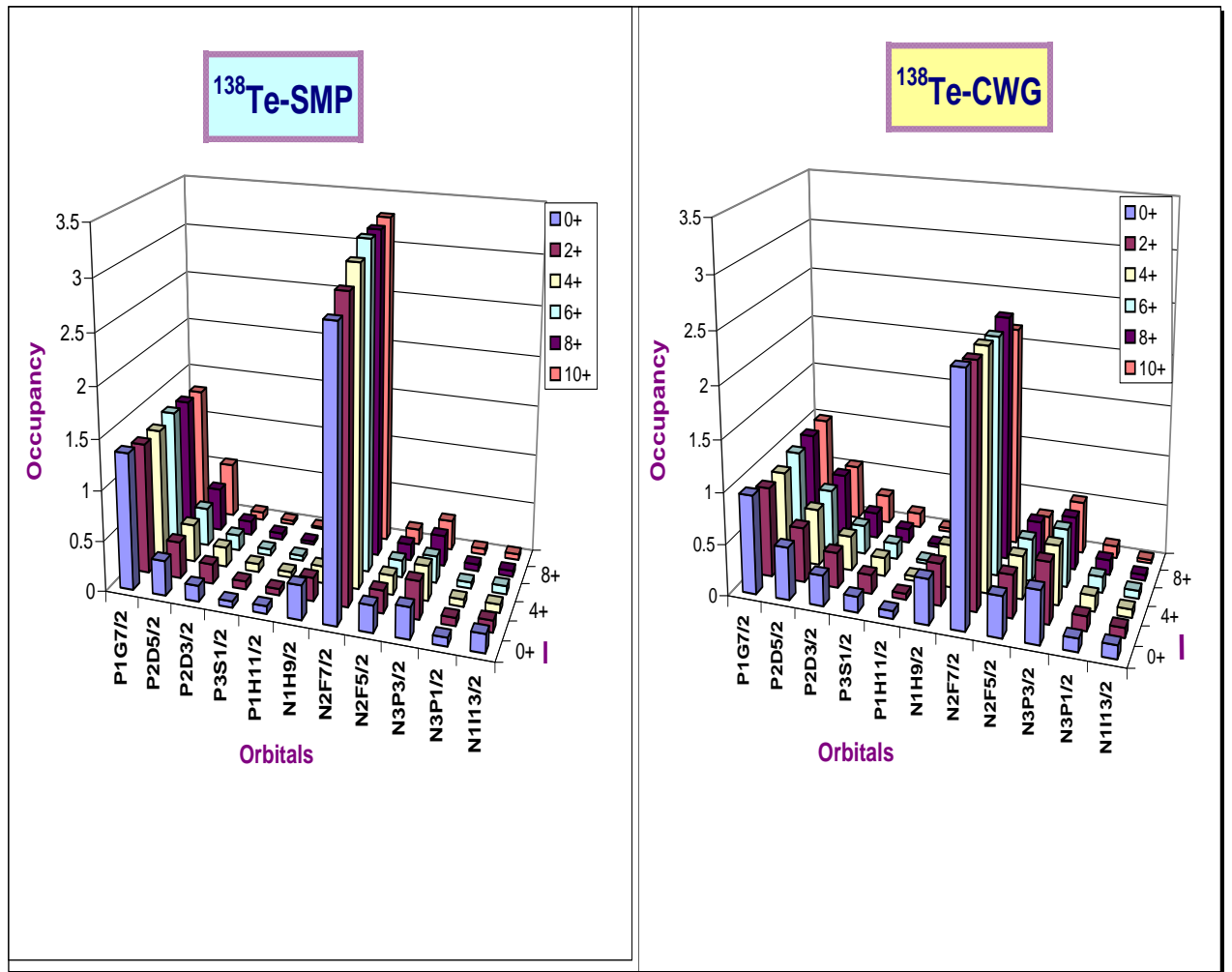


FIG. 10: (Color online) The plot of proton and neutron occupancies of different orbitals. See also the caption of Fig.9

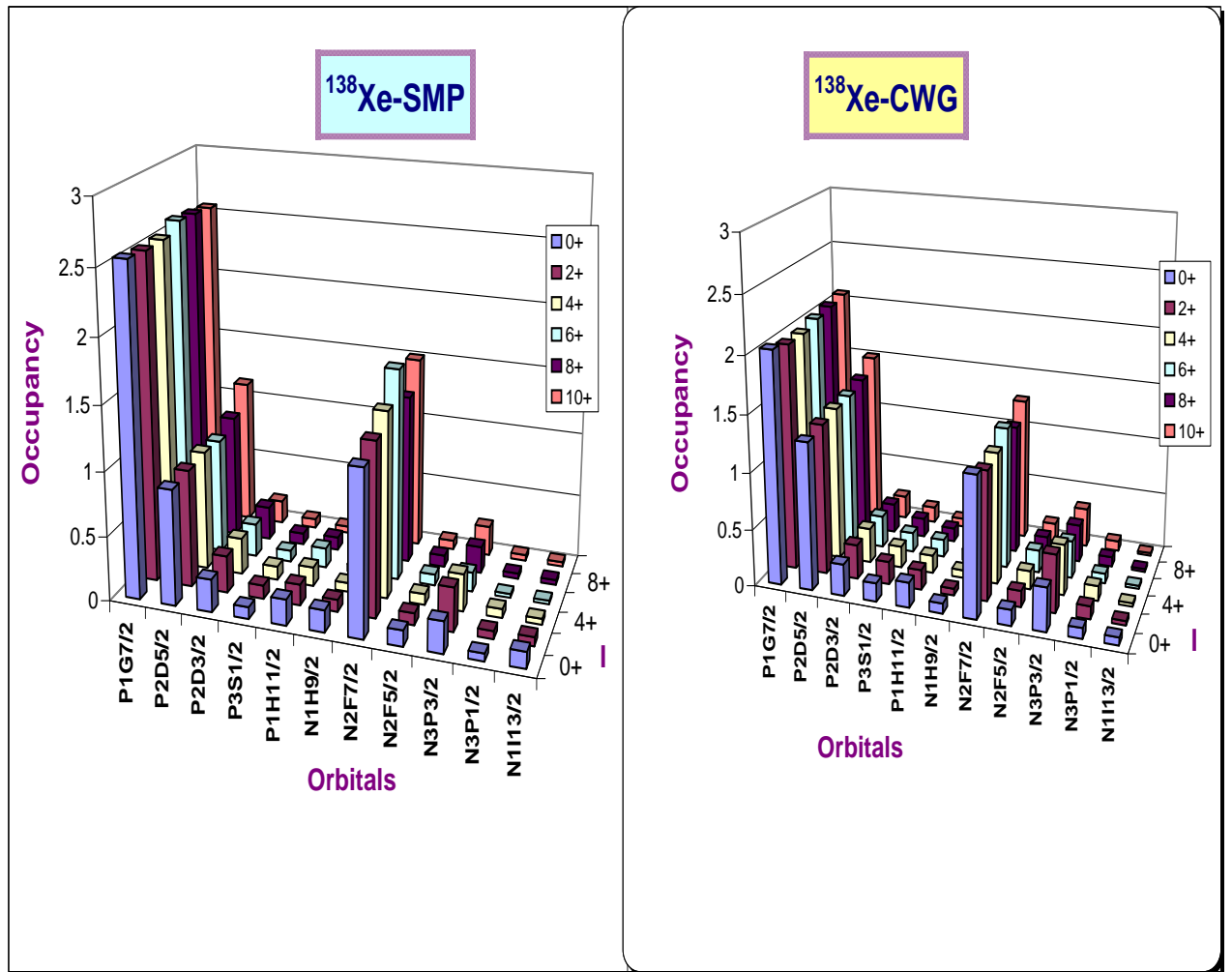


FIG. 11: (Color online) The plot of proton and neutron occupancies of different orbitals. See also the caption of Fig.9

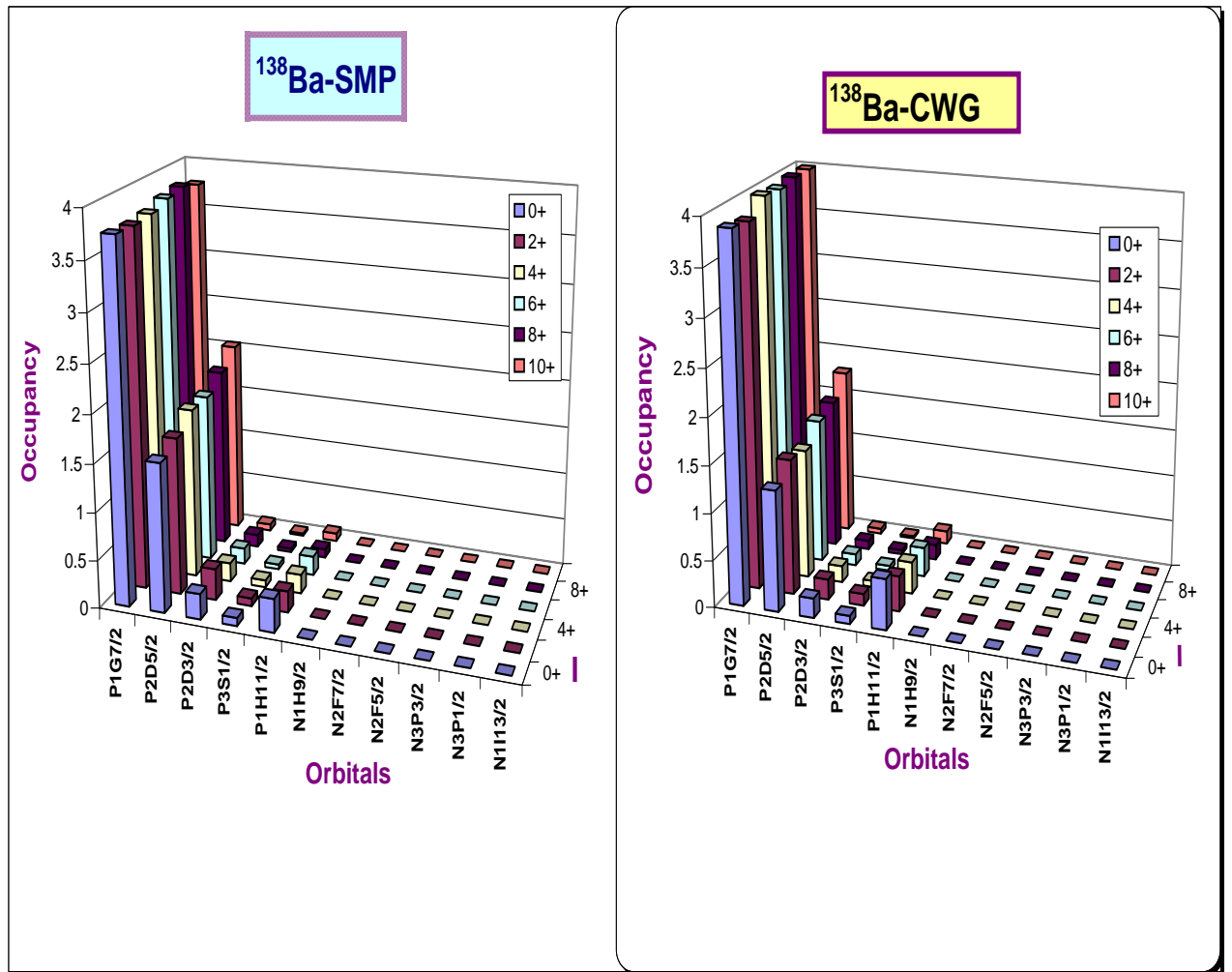


FIG. 12: (Color online) The plot of proton occupancies of different orbitals. See also the caption of Fig.9

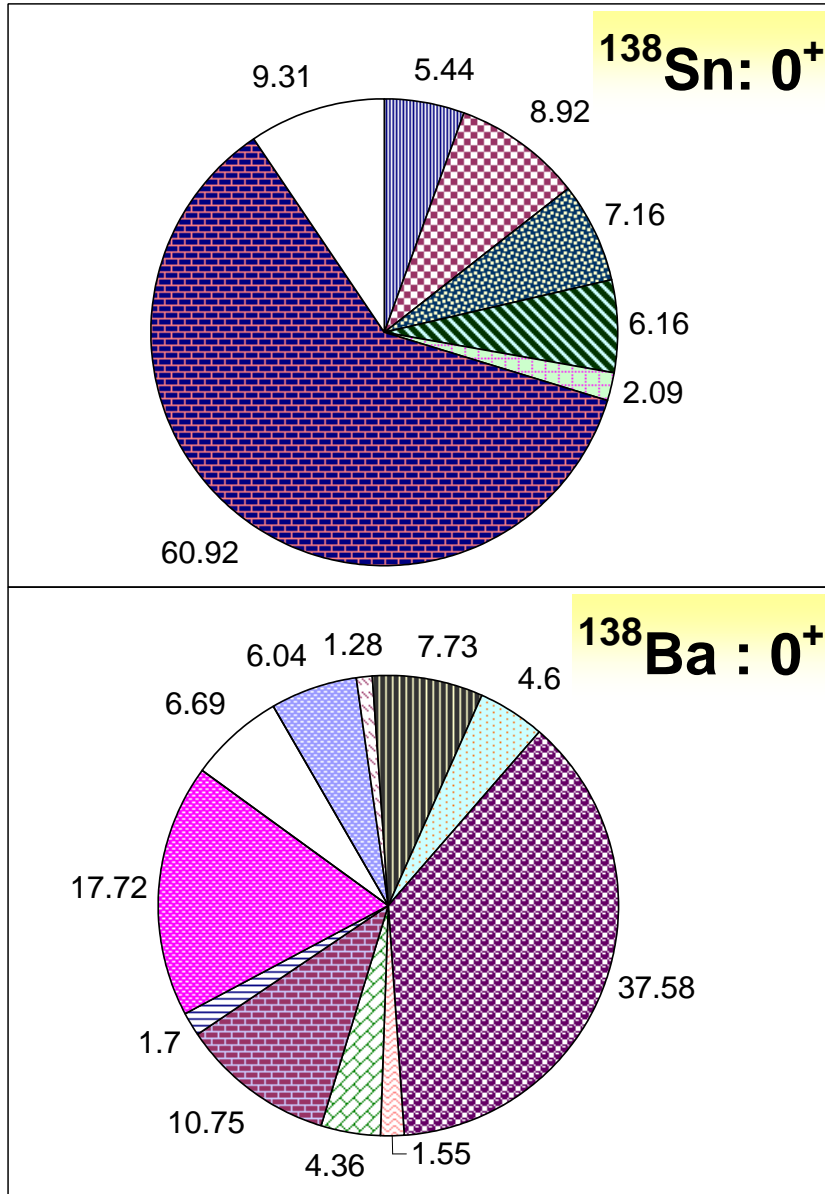


FIG. 13: (Color online) The  $\pi$ -chart plot of wavefunctions of the  $0_1^+$  states of  $^{138}\text{Sn}$  and  $^{138}\text{Ba}$ . The results are using the SMPN interaction. Numerical values associated with the different zones are the percentage (%) involvement of different particle - partitions composing the wave function. The zone marked white indicates the total contribution from all the partitions each of which contribute less than 1% in the wave function.

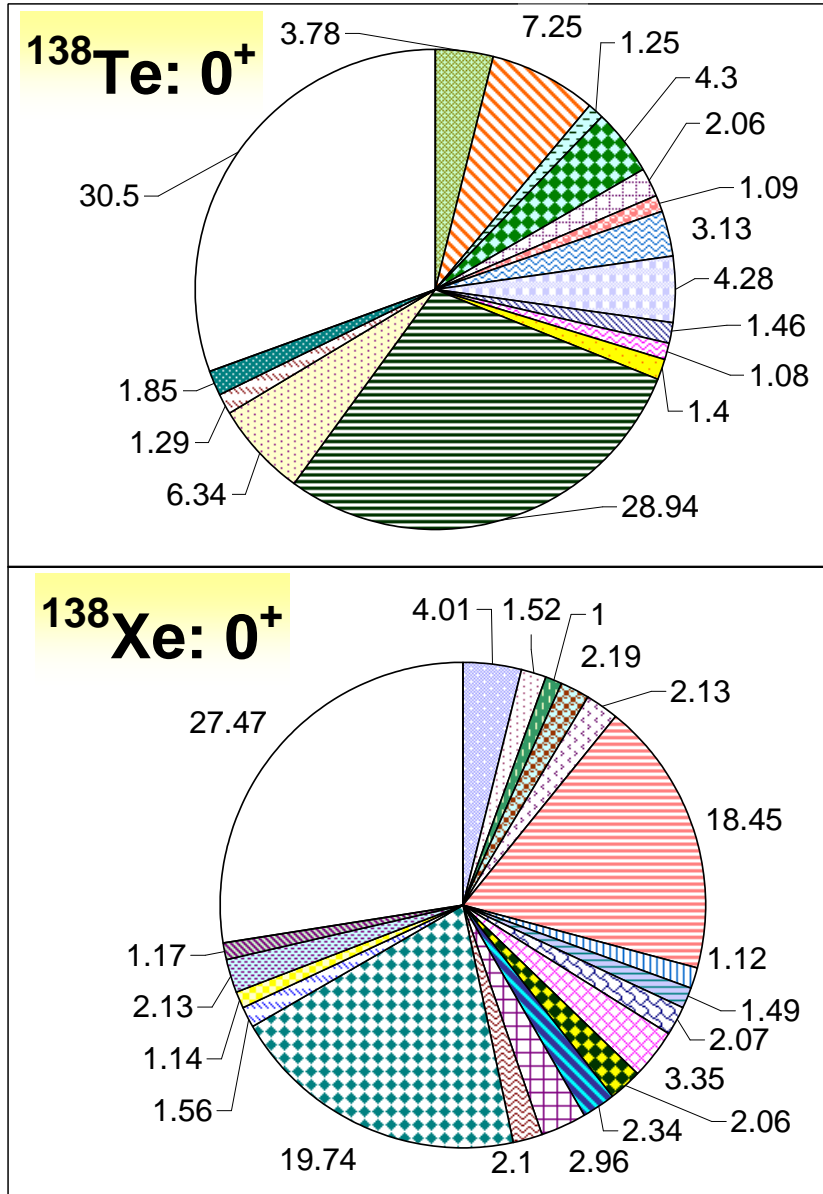


FIG. 14: (Color online) The  $\pi$ -chart plot of wavefunctions of the  $0_1^+$  states of  $^{138}\text{Te}$  and  $^{138}\text{Xe}$ . The results are using the SMPN interaction. See also the caption of Fig.13.